Tune optimization of the third generation light source storage ring based on Frequency Map Analysis*

TIAN Shun-Qiang(田顺强)[1,2;1)] LIU Gui-Min(刘桂民)[1] LI Hao-Hu(李浩虎)[1]
HOU Jie(后接)[1] ZHANG Wen-Zhi(张文志)[1]

1 (Shanghai Institute of Applied Physics, Chinese Academy of Sciences, Shanghai 201800, China)
2 (Graduate University of Chinese Academy of Sciences, Beijing 100049, China)

Abstract Tune optimization is necessary to optimize the nonlinearity of the third generation light source storage ring. In this paper we summarize the common strategies for choosing a tune and discuss tune optimization. Frequency Map Analysis (FMA) is applied as a tune scanning tool to reveal information about nonlinear resonances and guide the tune optimization. The Shanghai Synchrotron Radiation Facility (SSRF) storage ring is taken as a test lattice, and the optimum solutions are presented in this paper. Moreover, the third order regular structural resonances excited by sextupoles are particularly investigated, and it is found that these resonances distort the tune shifts with amplitude and show a stop-band like the linear structural resonances.

Key words storage ring, tune, FMA, structural resonance stop-band

PACS 29.20.dk, 41.85.-p, 42.65.-k

1 Introduction

The third generation light source is designed with very low emittance to provide photo output of high brightness[1—3]. The required strong quadrupoles entail very large natural chromaticity that must be compensated for by strong sextupoles. Nonlinearity corresponding to the sextupole drastically degrades the lattice acceptance. This fact makes nonlinear optimization indispensable in order to obtain an ample dynamic acceptance, and thus reach a long beam lifetime and efficient injection[4, 5]. Then a proper tune should be elaborately selected to make the nonlinear optimization much easier and more efficient, while also meeting the requirements of machine performance.

The brief criteria for choosing the tune could be[6—9]: (1) Providing enough focusing for low emittance; (2) Setting small β functions in the center of the straight section for minimizing beam size; (3) Having an integer part clear of linear structural resonances; (4) Having a fractional part less than 0.5 for suppressing the resistive wall instability; (5) Considering the nonlinear structural resonances, etc.

In the following sections we take the Shanghai Synchrotron Radiation Facility(SSRF) storage ring[10] as a test lattice to discuss the details. Optimization of the fractional part of the tune is emphasized. The tune diagram is commonly used to select a quiet working point[11], where the low order super-periodic structural resonances are considered, including skew and normal resonances. However, this method can't provide information about the resonance strength or stop-band. The tune diagram of the SSRF storage ring can be taken as an example, as shown Fig. 1, where the resonances are considered up to the sixth order, and A is the schematic for normal structural resonances, B for the normal and the skew structural resonances, and C contains all the possible resonances, including structural ones and non-structural ones. One can easily select a tune from A or B, but sometimes the non-structural resonances may have an unwanted effect on the beam dynamics. If one turns to C, it is difficult to select

Received 13 June 2008
* Supported by SSRF Project
1) E-mail: tianshunqiang@sinap.ac.cn

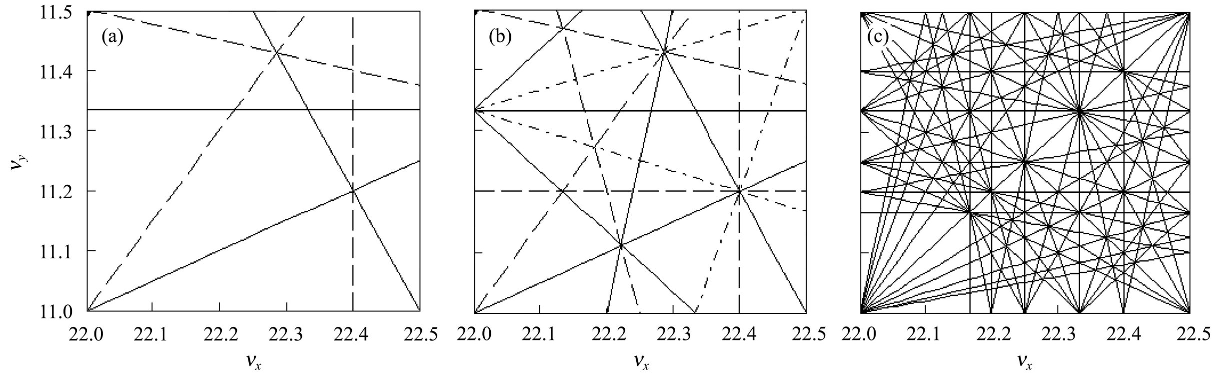

Fig. 1. Tune diagrams of the SSRF storage ring, just considering the tune zone of 22,11 (H,V), with a fractional part less than 0.5.

a tune. On the other hand, the low order resonance may have less effect on the global dynamics of the lattice, but the high order may strongly affect the dynamics. Tune optimization applied with the tune diagram usually leads into ambiguity.

Frequency Map Analysis (FMA)[12, 13] builds one-to-one maps between action and frequency, and applies tune shift with amplitude and tune diffusion with time to reveal the fine structure of the nonlinear resonances inside the dynamic aperture and provide qualitative information about these resonances. The additional information can be used to understand the mechanism of beam loss and guide the nonlinear optimization and the tune optimization. It has been extensively applied in many synchrotron light sources, such as ALS DIAMOND SOLEIL NSLS-Ⅱ et al.[14—17]. Some studies about tune optimization in the SSRF storage ring based on FMA have been reported in Refs. [8, 18]. In this paper, we take FMA as a tune scanning method to select a large quiet tune zone, which is relatively free of serious nonlinear resonance. The optimum solution of the SSRF storage ring has a dynamic aperture with a clear interior, which is beneficial for injection, and is tolerable to the tune shift in realistic operation, avoiding dropping into strong resonances. The details of the applications are presented in Section 3 and Section 4.

The first and second order structural resonances (linear structural resonances) are identified to show stop-bands and are regarded as the most dangerous resonances. If the tune is very close to these resonances, the lattice will have unstable optics. Intensive investigations on the linear structural resonances and their effect on the beam property have been reported in Refs. [19, 20]. In our studies it is revealed that the sextupole excited structural resonances (the third order normal structural resonances) still show a stop-band on the tune shift with amplitude. If the tune is on these resonances, the lattice may have stable optics. Even so, they must lead the particles with large oscillation amplitude into an island or degrade the dynamic aperture. This phenomenon will affect the beam lifetime and injection efficiency. Section 6 summarizes the theoretic analysis and simulation results with FMA.

In this paper all the simulative results are from the Accelerator Toolbox (AT)[21] code in the MATLAB environment.

2 Choosing the tune of the SSRF storage ring

The SSRF storage ring consists of 20 Double Bend Achromatic (DBA) cells with four super-periods. Each super-period contains three standard cells and two matching cells. There are 200 quadrupoles to adjust the linear optics and 140 sextupoles to compensate for the chromaticity all over the ring. The quadrupoles are classified into ten families but excited by individual power supply. The sextupoles are classified into eight families and excited family-by-family, in which two families are chromatic sextupoles and six families are harmonic sextupoles.

Generally, in the lattice with DBA cells, the phase advance of one cell is matched to 2π in the horizontal plane and π in the vertical plane. This case will have partial cancellation of the nonlinear driving forces generated by the sextupoles and easily obtain a better nonlinear behavior. Moreover, the stronger focusing, which is required to give phase advances of slightly more than 2π in the horizontal and more than π in the vertical, easily provide a low emittance, and reduce the β functions in the centers of the straight sections in order that the beam size can decrease in the forward. So the tune of the SSRF storage ring should be slightly larger than 20 in the horizontal plane and larger than 10 in the vertical plane. In these situations, a low emittance of about 4nm.rad can be easily obtained when the beam energy is 3.5 GeV.

A feasible tune should avoid dangerous resonances. The structural resonances in the lattice with the super-period may occur when the following condition is satisfied:

$$N_x\nu_x + N_y\nu_y = MP \ , \tag{1}$$

where N_x, N_y, M and P are integers, $|N_x|+|N_y|$ denotes the order of the resonance, M is the number of the super-period, and P is the harmonic number. The linear structural resonances can lead to unstable optics in the lattice, so the tune should depart from these resonances. In the previous study, the second order structural resonances showed a stop-band to break the β function, though this fact also allows the integer part of the tune to be that number where the second order structural resonance may occur[20]. As discussed, the integer part of the tune of the SSRF storage ring can be set to 21, 22 and 23 for the horizontal plane, and 10, 11 for the vertical plane. In the following sections, we select the 22, 11 and 23, 11 (H, V) tune zones for further investigation. In order to suppress the resistive wall instability, the fraction of the tune is set to less than 0.5.

3 Tune scan with frequency maps

In the storage ring, the motions of particles are perturbed by the sextupoles, and become a non-degenerate system with perturbation. KAM's theorem[22] asserts that for a sufficiently small perturbation, there still exists a Cantor set of values of ν, satisfying a Diophantine condition, for which the system still possesses smooth invariant tori with linear flow. In other words, there still exists a one-to-one smooth map from action variables (I) to frequency (ν):

$$F : I \to \nu \ , \tag{2}$$

and the tori are also described by I or by ν. One can search for a quasi-periodic approximation of the particle motion using turn-by-turn data with different initial condition variables to find the oscillation fundamental frequency, and apply tune shifts with amplitude and tune diffusions with time to reveal the fine structure of the resonances inside the dynamic aperture.

A tune scan with FMA can be carried out with two strategies. The first one is scanning in the vicinity of a reference working point with its frequency maps, and the better tunes can be found out. It has been discussed in Ref. [18]. The second one is carried out by the frequency maps of a series of matched tunes in a large zone. All the serious resonances in this zone can be revealed, and the quietest tunes can be directly selected. Fig. 2 shows the scanning results in two tune zones with on integer part of 22, 11 and 23, 11 (H, V), and a fractional part less than 0.5. The vertical tunes have a small interval (0.01), and the horizontal tunes have a large interval (0.05). This consideration is for covering the whole zone with less matched tunes. All the tunes are matched to the ideal symmetry and period, and the chromaticities are corrected to zero for both transversal planes only by the chromatic sextupoles. We have not considered the nonlinear optimization with harmonic sextupoles, because if the lattice has a large dynamic aperture, the scanning process will cost a lot of time. Each point is tracked for 1000 turns, and the tune diffusion is calculated with the difference of the frequency between the former 500 turns and the latter 500 turns, shown as grey shading from white for very stable motion to black for very unstable motion.

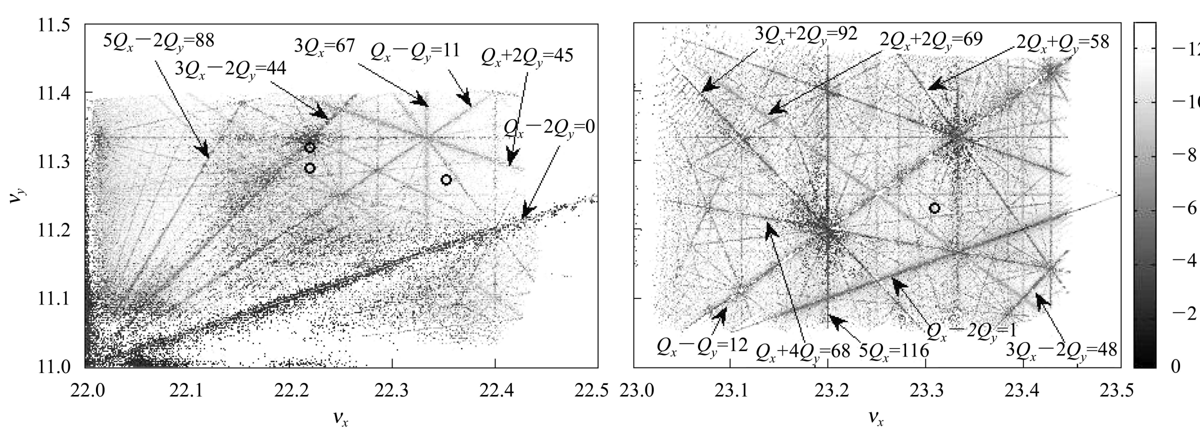

Fig. 2. Tune scanning with FMA in the zones of 22,11 (left figure) and 23,11 (right figure); 'o' denotes some investigated tunes.

The remarkable nonlinear resonances and the crosses are identified qualitatively, as shown in Fig. 2. The results guide the tune choosing without ambiguous findings in the tune diagram. The sextupole excited structural resonance Q_x-2Q_y=0 has a bad impact on the global dynamics of the ring. Further analysis is carried out in Section 6. With the information revealed by these figures, it is found that the nominal working point (Q_x,Q_y = 22.22, 11.32) of the SSRF storage ring is close to a serious structural resonance $3Q_x-2Q_y$ = 44. The same result is reported in Ref. [8], and it is explained that it is affected by the harmonic of the second order structural resonance stop-band Q_x=22. This fifth order structural resonance may lead to a loss of the injected beam. So, a more quiet working point should be selected for the realistic operation of the SSRF. Two new working points in the tune zone of 22, 11 are selected, i. e. 22.22, 11.29 and 22.353, 11.272. In the tune zone of 23, 11, a working point of 23.31, 11.23 is selected as the optimum result. The nonlinear optimization and the investigation of nonlinearities of these optimum tunes are presented in Section 4.

With the above results, it can be realized that the following resonances have a bad effect on the global dynamical property of the lattice, shown in Fig. 3, and the working point of the storage ring should be separate from these resonances: (1) The second order coupling resonances; (2) The third order regular resonances excited by normal sextuples, especially the structural ones; (3) The higher order regular structural resonances up to the sixth order.

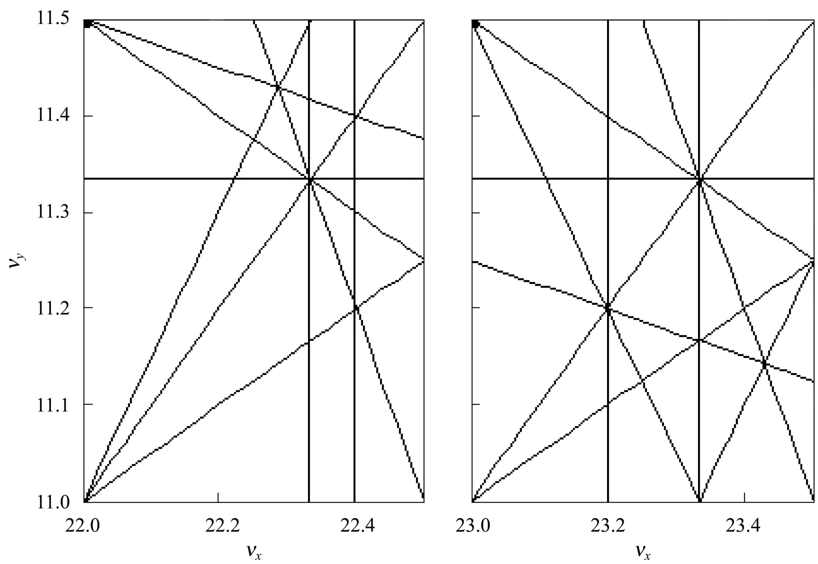

Fig. 3. The most remarkable resonances in the two tune zones.

Although the simulations in this section didn't consider the harmonic compensation, it should be envisaged that with the nonlinear optimization of the harmonic sextupoles it is still difficult to suppress the effect of these strong resonances. A lattice with a working point separate from these resonances can be expected to have a relatively clear dynamic aperture and frequency maps. Certainly, some other nonlinear resonances may appear in the dynamic aperture, but they are weak.

4 Tune optimization results

In Section 3, three working points, (Ⅰ) 22.22, 11.29 (Ⅱ) 22.353, 11.272 (Ⅲ) 23.31, 11.23, in the tune zones of 22, 11 and 23, 11 are selected as the tune optimization results, in which 22.22, 11.29 has been studied in Ref. [18], and has been successfully commissioned in the SSRF. In this section, the nonlinear optimizations and nonlinearities of the lattice with Tunes Ⅱ and Ⅲ will be introduced.

The linear optics of the two tunes are matched with the ideal symmetry and super-period, and in both cases the natural emittance is approximately 3.9 nm·rad, when the beam energy is 3.5 GeV. The harmonic sextupoles are optimized to reach a big on-momentum dynamic aperture, and the chromatic sextupoles correct the chromaticity to zero in both transversal planes. It is important to minimize the tune shift with amplitude in order to avoid bringing the particles with large amplitude into the most serious nonlinear resonances. Fig. 4 shows the tracking

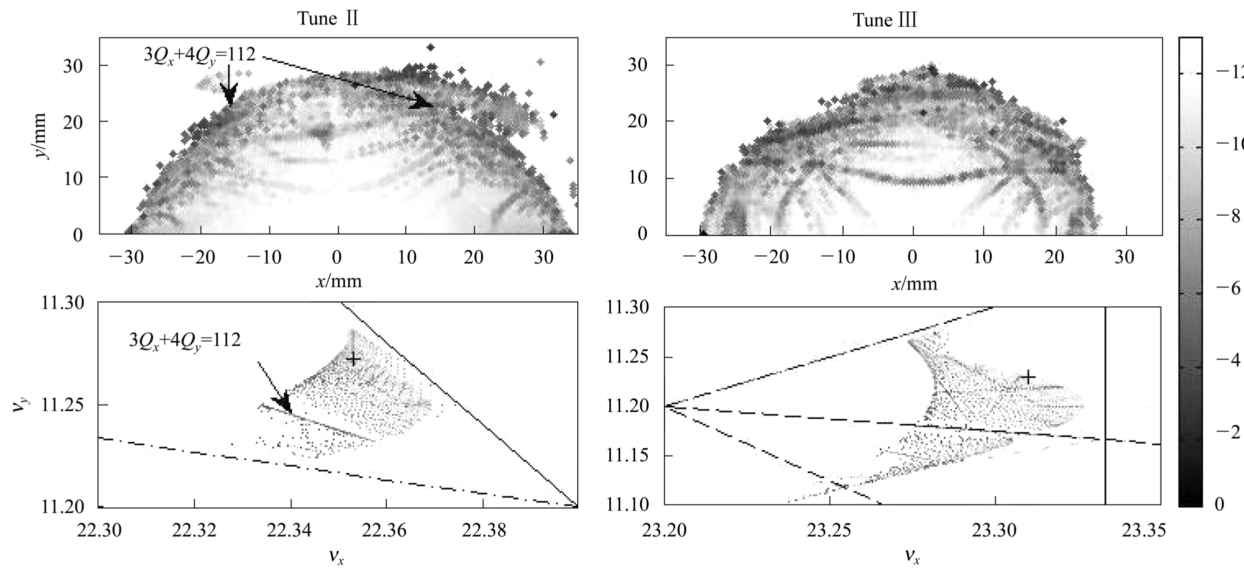

Fig. 4. Dynamic apertures and frequency maps of on-momentum particles of the lattice. The left two figures are for 22.353, 11.272, and the right two figures are for 23.31, 11.23.

results of the dynamic apertures and frequency maps of the Tunes Ⅱ and Ⅲ. It shows that the interior of the dynamic aperture of Tune Ⅱ is very clear and is hardly affected by any nonlinear resonance. Just a seventh structural resonance ($3Q_x+4Q_y=112$) seems to restrict its dynamic aperture. Some weaker resonances appear in the horizontal dynamic aperture of Tune Ⅱ. Even so, the result is acceptable.

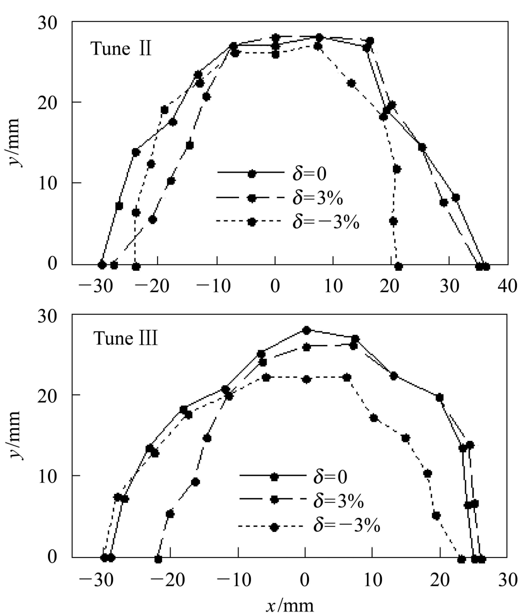

Fig. 5. Dynamic apertures of on- and off-momentum particles of the two tunes.

Figure 5 shows a scheme for the dynamic apertures of on- and off-momentum particles of the two tunes, which are tracked for 1000 turns. The lattice doesn't consider any magnetic error, and ignores radiation loss or beam energy compensation. The two tunes have ample dynamic acceptances to reach a long beam lifetime and efficient injection, and can be operated in the SSRF storage ring.

5 A new mode with lower emittance in the SSRF storage ring

In the tune zone of 23, 11, since there is stronger focusing than in the zone of 22, 11, a new mode with lower emittance can be designed. The tune is selected to be 23.324, 11.232. It can be expected that the natural chromaticity will become large, and thus be corrected by stronger chromatic sextupoles. The corresponding nonlinearity of the sextupoles will degrade the lattice acceptance more than the nominal mode, so β_x in the center of the long straight section is matched to 12 m in order to get an ample horizontal dynamic aperture for efficient injection. The matched β functions in the center of the standard straight section are reduced in order to provide the additional phase advances and obtain a smaller beam size. Then an emittance of 3.36 nm·rad with 3.5 GeV beam energy can be obtained.

The strengths of the harmonic sextupoles are elaborately optimized in order to obtain an ample dynamic aperture. The frequency maps and the dynamic aperture of on-momentum particles are depicted in Fig. 6, where a sixth structural resonance appears in the dynamic aperture, and affects the vertical plane. The dynamic apertures of off-momentum particles are showed in Fig. 7. The theoretic tune and nonlinear optimum results are acceptable, and the first commissioning in the SSRF storage ring is successful, when the beam energy is 3.0 GeV, and the natural emittance is 2.47 nm·rad.

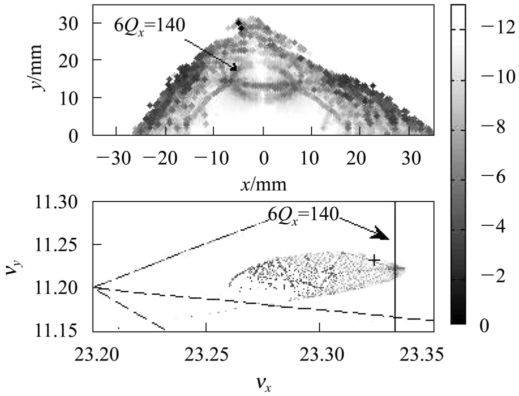

Fig. 6. Dynamic aperture and frequency maps of on-momentum particles of the lower emittance mode.

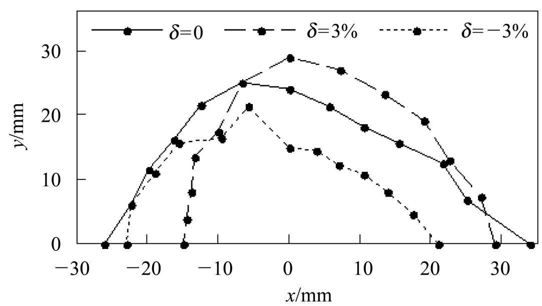

Fig. 7. Dynamic apertures of on- and off-momentum particles of the lower emittance mode.

6 Nonlinear resonances excited by sextupoles

From the tune scanning of the 22, 11 zone with FMA, as shown in Fig. 2, one notes that the third order regular structural resonance excited by sextupoles, $Q_x-2Q_y=0$, disturbs the frequency maps and shows a stop-band. It means that the tune shift with amplitude has a distortion when the oscillation frequency of the particle drops on or close to this resonance. It can be expected that if the working point is on or close to this resonance, the dynamic aperture may be badly affected by it, and the large amplitude even be broken to form an isolated island. In the realistic operation of the machine, this phenomenon may lead to a loss of the injected beam or blow up the stored beam and make it de-coherent.

If only the second order (linear) tune shift terms with amplitude are considered, then the tune shift can be expressed by the following formula:

$$\begin{cases} \Delta\nu_x = 2J_x c_{11} + J_y c_{12} \\ \Delta\nu_y = 2J_y c_{22} + J_x c_{12} \end{cases}, \tag{3}$$

where $J_z=(\beta_z\varepsilon_z)^{1/2}$ for $z=x,y$ and the nonlinear coefficients c_{ij} are functions of the optics and the sextupole strengths. They can be calculated with the following formula[23]:

$$c_{11} = \frac{\partial\nu_x}{\partial J_x} = -\frac{1}{16\pi}\sum_{j=1}^{N}\sum_{k=1}^{N}(b_3L)_j(b_3L)_k\beta_{xj}^{3/2}\beta_{xk}^{3/2}\times\left[\frac{3\cos(|\mu_{j\to k,x}|-\pi\nu_x)}{\sin(\pi\nu_x)}+\frac{\cos(|3\mu_{j\to k,x}|-3\pi\nu_x)}{\sin(3\pi\nu_x)}\right], \tag{4}$$

$$c_{12} = \frac{\partial\nu_x}{\partial J_y} = \frac{1}{8\pi}\sum_{j=1}^{N}\sum_{k=1}^{N}(b_3L)_j(b_3L)_k\sqrt{\beta_{xj}\beta_{xk}}\beta_{yj}\left[\frac{2\beta_{xk}\cos(|\mu_{j\to k,x}|-\pi\nu_x)}{\sin(\pi\nu_x)}+\frac{\beta_{yk}\cos[|\mu_{j\to k,x}+2\mu_{j\to k,y}|-\pi(\nu_x+2\nu_y)]}{\sin\pi(\nu_x+2\nu_y)}+\frac{\beta_{yk}\cos[|\mu_{j\to k,x}-2\mu_{j\to k,y}|-\pi(\nu_x-2\nu_y)]}{\sin\pi(\nu_x-2\nu_y)}\right], \tag{5}$$

$$c_{22} = \frac{\partial\nu_y}{\partial J_y} = -\frac{1}{16\pi}\sum_{j=1}^{N}\sum_{k=1}^{N}(b_3L)_j(b_3L)_k\sqrt{\beta_{xj}\beta_{xk}}\beta_{yj}\beta_{yk}\left[\frac{4\cos(|\mu_{j\to k,x}|-\pi\nu_x)}{\sin(\pi\nu_x)}+\frac{\cos[|\mu_{j\to k,x}+2\mu_{j\to k,y}|-\pi(\nu_x+2\nu_y)]}{\sin\pi(\nu_x+2\nu_y)}+\frac{\cos[|\mu_{j\to k,x}-2\mu_{j\to k,y}|-\pi(\nu_x-2\nu_y)]}{\sin\pi(\nu_x-2\nu_y)}\right], \tag{6}$$

where j, k denote the sextupole index, $\mu_{j\to k}$ is the phase advance from the j-th sextupole to the k-th sextupole, and β, ν are the beta function and the tune. If situations with $\nu_x=p$ and $3\nu_x=p$ occur, function c_{11} is undefined, and for situations with $\nu_x=p$ and $\nu_x\pm 2\nu_y=p$, the functions c_{12} and c_{22} are undefined, where p is a multiple of 4 for the SSRF storage ring. Fig. 8 plots the tree coefficients as a function of the tune in the 22, 11 zone, where the harmonic compensations are still ignored. One recognizes the distortions of these coefficients. This fact causes a large aberration for the corresponding frequency, and thus restricts the dynamic aperture. Fig. 9 plots the dynamic aperture areas of different tunes, in which the fact that the dynamic aperture is restricted by $Q_x - 2Q_y = 0$ is validated. These phenomenons are not found in the tune zone of 23, 11, because there is not any third order regular structural resonance.

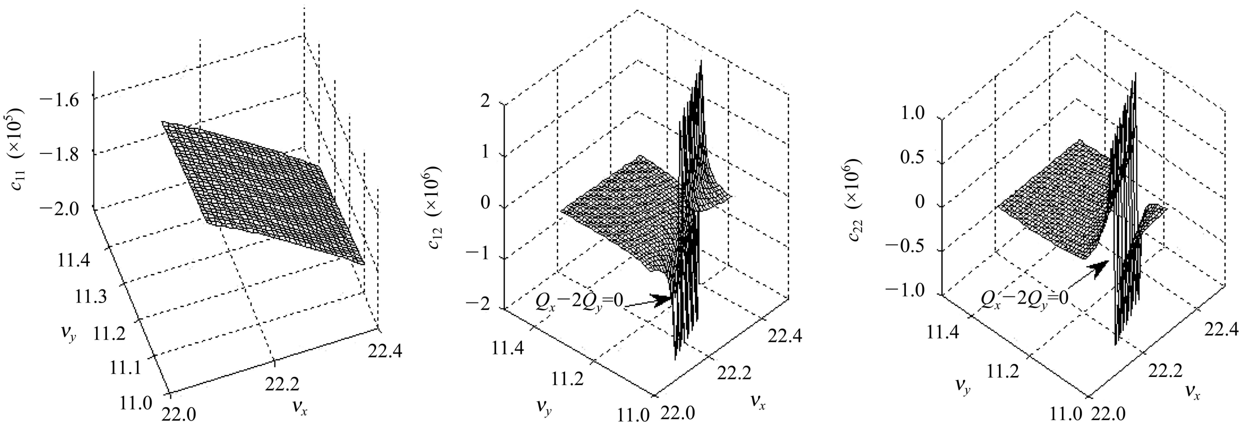

Fig. 8. Linear tune shift coefficients with amplitude as a function of the matched tune.

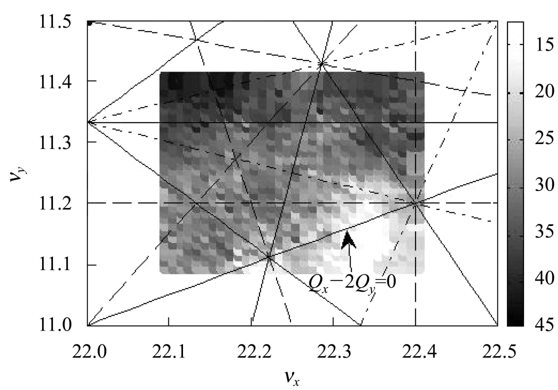

Fig. 9. Areas of the dynamic aperture as a function of tune, without harmonic sextupole compensation.

The results presented above are obtained without considering harmonic sextupole compensations. Nonlinear optimization for the strengths of harmonic sextupoles usually applies a convergent algorithm, in which some penalty function forces convergence to a minimum within one turn map, and then one expects to obtain a large dynamic acceptance. In a complex lattice with low symmetry, such as the SSRF storage ring, the penalty function must contain the linear tune shift terms. So, if the tune is on or close to any third order regular structural resonance, the convergence for the penalty function may be defeated, or no ample dynamic acceptance can be obtained. On the other hand, if the frequency of the particle with large amplitude drops into these resonances, the particle may be lost or be in an isolated island.

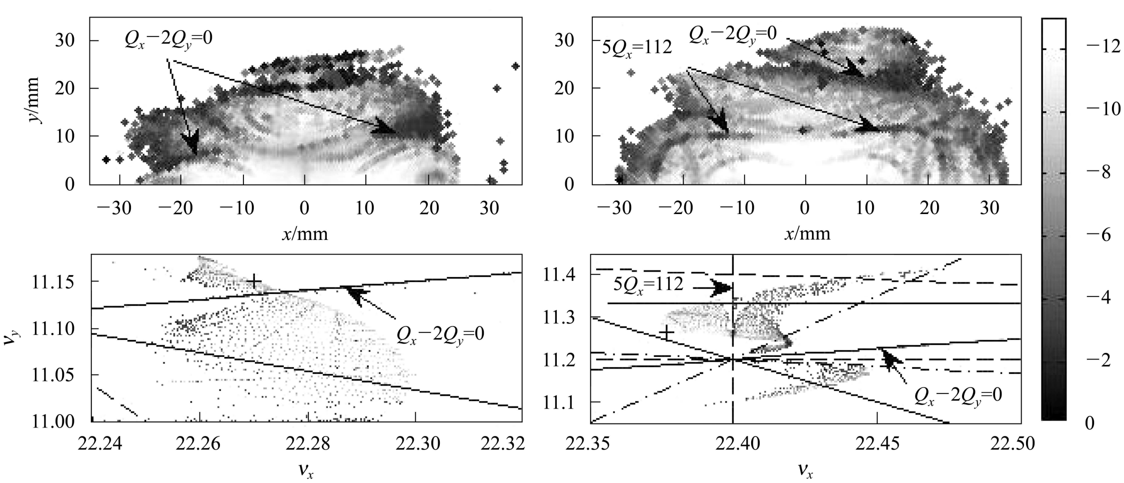

Fig. 10. Dynamic apertures and frequency maps of the tune 22.27, 11.15 (left two figures) and 22.377, 11.264 (right two figures). They show the effect of $Q_x - 2Q_y = 0$.

Figure 10 shows two examples. The left two figures are the dynamic aperture and the frequency maps for the tune 22.27, 11.15 and the right two figures are for the tune of 22.377, 11.264. The tune 22.27, 11.15 is very close to $Q_x - 2Q_y = 0$. It makes nonlinear optimization very difficult, so no ample dynamic aperture can be provided. The figures show that $Q_x - 2Q_y = 0$ divides the frequency maps, and makes the particles with vertical amplitudes larger than 5 mm almost drop into an isolated island. The tune 22.377, 11.264 is far away from $Q_x-2Q_y=0$, and it is in a quiet zone as shown in the left part of Fig. 2. Unfortunately, some particles with large vertical amplitude are in an isolated island due to the effect of $Q_x - 2Q_y=0$. Another remarkable resonance inside the dynamic aperture is $5Q_x=112$, which is summarized in Fig. 3, and should be taken into account in tune choosing.

7 Conclusions

The common strategies for the tune choosing of the third generation light source storage ring are discussed. Frequency map analysis was applied as a tune scanning tool to optimize the fractional part of the tune. The SSRF storage ring is taken as a test lattice, and its tune optimizations are discussed in details. Two tune zones, whose integer parts are 22, 11 and 23, 11 with the fractional part less than 0.5, are selected in order to reach low emittance and good nonlinear performances. The most dangerous resonances are revealed with the application of FMA, and its universal principles are extracted which should be elaborately considered in the tune optimization of the complex lattice. Some optimum tunes are given that provide a large dynamic aperture and better nonlinear performance. A new mode of the SSRF storage ring with lower emittance is designed in the tune zone of 23, 11. The third order regular structural resonances excited by sextupoles make the linear tune shift with amplitude highly distorted. This fact is validated by FMA. When the tune is on or close to these resonances with the large tune shifts, it is difficult to optimize the nonlinearity of the lattice, and thus no sufficient dynamic acceptance can be obtained. Another effect of these resonances is to lead the particles with large amplitudes to drop into an isolated island, and to be easily lost in the realistic operation of the light source.

References

1 Corbett Jeff. Rabedeau Thomas. Nucl. Instrum. Methods A, 2003, **500**: 11
2 Lee Tae-Yeon, Choi Jinhyuk. Nucl. Instrum. Methods A, 2003, **515**: 410
3 Gladkikh P I, Karnaukhov I M, Kononenko S G et al.Nucl. Instrum. Methods A, 2000, **448**: 41
4 Laclare J L. Nucl. Instrum. Methods A, 2001, **467-468**: 1
5 Bengtsson J, Joho W, Marchand P et al. Nucl. Instrum. Methods A, 1998, **404**: 237
6 Smith S L. Proceedings of the European Particle Accelerator Conference. France: Paris, 2002. 44—48
7 Owen H, Jones J, Smith S. Proceedings of the European Particle Accelerator Conference. France: Paris, 2002. 751—753
8 JIAO Y, FANG S X, QIN Q et al. Nucl. Instrum. Methods A, 2006, **566**: 270
9 Sacherer F. Proc. of 9th Int. Conf. on High Energy Accelerators. 1974. 347—349
10 LIU Gui-Min, DAI Zhi-Min, LI Hao-Hu et al. HEP&NP, 2006, **30**(Supp. I): 144 (in Chinese)
11 Robin D. Phys. Rev. ST, 1999, **2**: 044001
12 Dumas H S, Laskar J. Phys. Rev. Lett., 1993, **70**: 2975
13 Laskar J. Proceedings of the Particle Accelerator Conference. USA: Portland, Oregon, 2003. 378—382
14 Sterier C, Robin D, Nadolski L et al. Phys. Rev. E, 2002, **65**: 056506
15 Belgroune M, Baldwin A I, Bartolini R et al. Proceedings of the Particle Accelerator Conference. Knoxville, Tennessee, USA: 2005, 1410—1412
16 Belgroune M, Brunelle P, Laskar J et al. Proceedings of the European Particle Accelerator Conference. Paris, France: 2002, 1229—1231
17 Bengtsson J. Proceedings of the European Particle Accelerator Conference. Edinburgh, Scotland: 2006, 3478—3480
18 TIAN Shun-Qiang, LIU Gui-Min, LI Hao-Hu et al. Chinese Physics C (HEP & NP), 2009, **33**(2): 127
19 FANG Shou-Xian, QIN Qing. HEP&NP, 2006, **30**(9): 880
20 TIAN Shun-Qiang, HOU Jie, CHEN Guang-Ling et al. Chinese Physics C, 2008, **32**(7): 576
21 Terebilo A. Accelerator Toolbox for MATLAB, SLAC-PUB-8732
22 Arbold V I, Kozlov V V, Neishtadt A I. Mathematical Aspects of Classical and Celestial Mechanics, Dyn. Systems III. Arnold V I, ed. Springer, New York: 1988
23 Bengtsson J. The Sextupole Scheme for the Swiss Light Source, SLS Note 9/97